2023 62nd IEEE Conference on Decision and Control (CDC)
December 13-15, 2023. Marina Bay Sands, Singapore

Cooperative Lane Changing in Mixed Traffic Can Be Robust to Human Driver Behavior

Anni Li, Andres S. Chavez Armijos, and Christos G. Cassandras

***Abstract*— We derive time and energy-optimal control policies for a Connected Autonomous Vehicle (CAV) to complete lane change maneuvers in mixed traffic. The interaction between CAVs and Human-Driven Vehicles (HDVs) requires the best possible response from a CAV to actions by its neighboring HDVs. This interaction is formulated using a bilevel optimization setting with an appropriate behavioral model for an HDV. An iterated best response (IBR) method is then used to determine a Nash equilibrium. However, we also show that CAV cooperation can eliminate or greatly reduce the interaction between CAVs and HDVs. We derive a simple threshold-based criterion to select an optimal policy for the lane-changing CAV to merge ahead of a cooperating CAV in the target lane. In this case, the trajectory of the lane-changing CAV is independent of HDV behavior. Simulation results are included to demonstrate the effectiveness of our CAV controllers in terms of minimizing cost and disruption to traffic flow while guaranteeing safety when uncontrollable HDVs are present.**

I. INTRODUCTION

The emergence of Connected Autonomous Vehicles (CAVs) has the potential to significantly transform transportation networks and enhance their performance. CAVs can assist drivers in making decisions that reduce travel times, energy consumption, air pollution, traffic congestion, and accidents. In the context of highway driving, this potential is realized in automating lane-changing maneuvers through proper trajectory planning [1] or by accelerating maneuver evaluation using car-following models [2]. However, executing a lane change maneuver often requires cooperation from other vehicles, especially in heavy traffic conditions [3]. The cooperation among CAVs offers opportunities for safely [4] and optimally [5] performing automated lane change maneuvers.

Since achieving 100% CAV penetration in the near future is unlikely, a crucial question arises: how can we benefit from the presence of at least some CAVs in mixed traffic, where CAVs must interact with human-driven vehicles (HDV)? This question has become the focal point of recent research.

For instance, researchers have developed adaptive cruise controllers for mixed traffic environments, employing platoon formulations for CAVs [6]. Car-following models have been implemented to provide a deterministic quantification of HDV states [7]. To accurately model HDV behavior, [8] introduced the concept of social value orientation for autonomous driving, quantifying an agent's degree of "prosocialness" or individualism and applying a game-theoretic formulation to predict human behavior. Vehicle interactions are considered in [9], [10], using bilevel optimization to assist autonomous vehicles in choosing the best possible response to an opponent's action. Similarly, learning-based techniques are applied in [11], [12].

In this paper, we consider the *joint time and energy-optimal* automated lane change problem in the presence of mixed traffic, while minimizing the overall *traffic throughput disruption*. Fig. 1 illustrates that vehicle cooperation cannot be guaranteed when the red vehicle is an HDV.

The primary contribution of this paper is the derivation of optimal lane-changing trajectories for vehicle C in Fig. 1 along the longitudinal traffic direction in a mixed traffic setting. Here, the two CAVs in the figure must interact with the HDV. We limit our analysis to these triplets since they allow two CAVs to cooperate while also interacting with the HDV. For C to merge ahead of the HDV safely, it must account for the driver's behavior, as the HDV is otherwise uncontrollable. Another option is for CAV C to merge ahead of the cooperating CAV 1, effectively constraining the HDV to "follow" CAV 1. we establish a game-theoretic framework for the interactive decision-making process between the CAVs and the HDV.

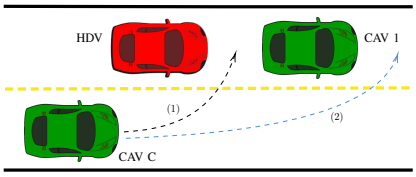

Fig. 1: The basic lane-changing maneuver process.

II. PROBLEM FORMULATION

The lane change maneuver is triggered by CAV C when it detects an obstacle ahead or at a time determined by the CAV. Our goal is to minimize maneuver duration and energy consumption while minimizing disruptions to fast lane traffic. Additionally, in the presence of HDVs, vehicle C must consider HDV behavior to ensure safety, necessitating HDV behavior estimation.

For each vehicle in Fig. 1, denoted by $i = 1, C, H$, their dynamics are described as:

$$\dot{x}_i(t) = v_i(t), \quad \dot{v}_i(t) = u_i(t) \tag{1}$$

Here, $x_i(t)$ denotes the current longitudinal position relative to a reference point, while $v_i(t)$ and $u_i(t)$ represent the speed and controllable acceleration of vehicle i at time

This work was supported in part by NSF under grants CNS-2149511, ECCS-1931600, DMS-1664644 and CNS-1645681, by ARPAE under grant DE-AR0001282, and by the MathWorks.

A. Li, A. S. Chavez Armijos, and C. G. Cassandras are with the Division of Systems Engineering and Center for Information and Systems Engineering, Boston University, Brookline, MA 02446 (email:{anlianni; aschavez; cgc}@bu.edu).

t, respectively. Actions for vehicles $1, C, H$ commence at time t_0, with $x_C(t_0)$ marking CAV C's initial position. The maneuver concludes at time t_f. Notably, we do not address the lateral component of the lane change in this paper. Vehicle C deals with lateral control, aiming to minimize time and energy consumption, akin to [13]. Lateral motion can also be managed using detailed models and auxiliary techniques like model predictive control (MPC), as discussed in [14].

The control inputs and speeds for all vehicles are subject to the following constraints:

$$u_{i_{\min}} \leq u_i(t) \leq u_{i_{\max}},\ v_{i_{\min}} \leq v_i(t) \leq v_{i_{\max}},\ \forall t \in [t_0, t_f] \quad (2)$$

Here, $u_{i_{\min}}$ and $u_{i_{\max}}$ represent the minimum and maximum allowable accelerations for vehicle i. Similarly, $v_{i_{\min}}$ and $v_{i_{\max}}$ denote the minimum and maximum allowable speeds for vehicle i, which are determined in accordance with established traffic rules.

Safety Constraints: The minimum safe following distance for each vehicle i, denoted as $d_i(v_i(t))$, is determined based on its speed relative to its preceding vehicle in the same lane:

$$d_i(v_i(t)) = \varphi v_i(t) + \delta \quad (3)$$

Here, φ is the reaction time (typically set as $\varphi = 1.8s$ [15]), and δ is a constant. $d_i(v_i(t))$ measures the distance from the center of vehicle i to the center of its preceding vehicle. All vehicles, including $i = 1, C, H$ in Fig. 1, must adhere to the following constraints to ensure safety during lane change maneuvers.

$$x_1(t) - x_H(t) \geq d_H(v_H(t)), \quad \forall t \in [t_0, t_f] \quad (4a)$$
$$x_C(t_f) - x_H(t_f) \geq d_H(v_H(t_f)), \quad (4b)$$
$$x_1(t_f) - x_C(t_f) \geq d_C(v_C(t_f)). \quad (4c)$$

where (4a) is the rear-end safety constraint between CAV 1 and the HDV for all $t \in [t_0, t_f]$, whereas (4b),(4c) provide safety guarantees that CAV C must satisfy only at t_f.

Traffic Disruption: We adopt the disruption metric introduced in [16] which includes both a position and a speed disruption. Each disruption metric is measured relative to its corresponding value under no maneuver. In particular, for any vehicle i, the position disruption d_x^i, speed disruption d_v^i, and total disruption $D_i(t)$ at time t are given by

$$d_x^i(t) = \begin{cases} (x_i(t) - \bar{x}_i(t))^2, & \text{if } x_i(t) < \bar{x}_i(t) \\ 0, & \text{otherwise.} \end{cases} \quad (5a)$$
$$d_v^i(t) = (v_i(t) - v_{d,i})^2 \quad (5b)$$
$$D_i(t) = \gamma_x d_x^i(t) + \gamma_v d_v^i(t) \quad (5c)$$

where $\bar{x}_i(t) = x_i(t_0) + v_i(t_0)(t - t_0)$ is the position of i when it maintains a constant speed $v_i(t_0)$ (note that if $x_i(t) \geq \bar{x}_i(t)$ we do not consider this as a traffic disruption since i has not decelerated). In the definition of $d_v^i(t)$, $v_{d,i} \leq v_{\max}$ is the desired speed of vehicle i which matches the fast lane traffic flow. The weights γ_x, γ_v are selected to form a convex combination emphasizing one or the other term to reflect the total disruption generated by vehicle i.

In the next two sections, for CAV C to merge ahead of HDV or CAV 1 is analyzed and the optimal trajectories are determined. By comparing the overall costs resulting from each decision, we may then determine the optimal option. We note that the latter maneuver can be executed *without any knowledge of the HDV behavior*; the only possible effect such a maneuver has on the HDV is causing some disruption if the HDV has to decelerate to maintain a safe distance from CAV 1.

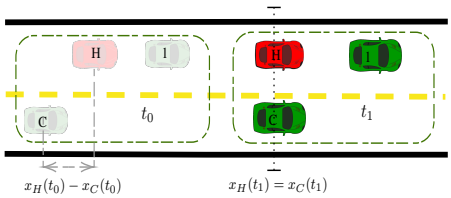

Fig. 2: The relative positions of 1, C, H at t_0 and t_1

III. CAV C MERGES AHEAD OF HDV

Let us assume that at the start of the maneuver t_0, we have $x_C(t_0) < x_H(t_0) < x_1(t_0)$. Thus, we begin by separating the maneuver into two phases, $[t_0, t_1)$ and $[t_1, t_f]$, where t_1 is defined as

$$t_1 = \min\{t \mid t \geq t_0,\ x_H(t) \leq x_C(t)\} \quad (6)$$

Thus, t_1 denotes the first time instant that the HDV considers any possible reaction to CAV C (if $x_C(t_0) \geq x_H(t_0)$, then $t_1 = t_0$). In other words, there is no interaction between CAV C and the HDV until t_1. The relative position of the triplet $(1, C, H)$ over the two phases is shown in Fig. 2. In Phase I, CAV C plans a trajectory that jointly minimizes t_1 and its energy consumption over $[t_0, t_1)$. In Phase II, CAV C estimates the behavior of the HDV and solves a bilevel optimization problem leading to a solution based on an iterated best response (IBR) algorithm.

A. Optimal Trajectory for CAV C in Phase I

Assuming that CAV 1 and the HDV travel with constant speed in Phase I, CAV C can solve the following optimal control problem termed $\mathbf{OCP}_{[t_0,t_1)}$:

$$J_1^I = \min_{t_1, u_C(t)} \int_{t_0}^{t_1} [\alpha_t + \frac{\alpha_u}{2} u_C^2(t)]dt + \alpha_v (v_C(t_1) - v_{d,C})^2 \quad (7a)$$
$$s.t.\ (1), (2)$$
$$x_C(t_1) = x_H(t_1) \quad (7b)$$
$$t_0 \leq t_1 \leq T \quad (7c)$$

The cost (7a) combines the travel time $t_1 - t_0$ and an energy term $u_C^2(t)$ along with a terminal cost on the speed $v_C(t_1)$, where $\alpha_{\{u,t,v\}}$ are adjustable non-negative properly normalized weights. Constraint (7b) follows from (6), and (7c) gives a maximum allowable time T for C to perform a lane change maneuver. If (7c) is violated, the maneuver is aborted at t_0.

However, $\mathbf{OCP}_{[t_0,t_1)}$ may be infeasible if the initial states are such that $v_H(t_0) > v_C(t_0)$, $x_H(t_0) > x_C(t_0)$ and the allowable maneuver time T is small. To allow for such possible infeasibility, we consider two additional policies

that CAV C can adopt. The first is to simply speed up with a constant acceleration $u_{i_{\max}}$ so that

$$u_C(t) = \begin{cases} u_{C_{\max}}, & \forall t \in [t_0, \frac{v_{C_{\max}} - v_C(t_0)}{u_{C_{\max}}}) \\ 0, & \forall t \in [\frac{v_{C_{\max}} - v_C(t_0)}{u_{C_{\max}}}, t_1) \end{cases} \quad (8)$$

which allows for the possibility that the maximum speed $v_{C_{\max}}$ is achieved before t_1, which is obtained from $x_C(t_1) = x_H(t_0) + v_H(t_0)(t_1 - t_0)$. Using the same cost function as (7a) with $u_C(t)$ in (8) we obtain the cost J_2^I for this constant acceleration policy.

The second alternative policy exploits the cooperation capabilities between CAVs, so that CAV 1 may decelerate to induce a deceleration of the HDV due to the safety requirement (4a). If the HDV decelerates, the time for C to catch up with the HDV is reduced. The resulting OCP can be formulated as

$$J_3^I = \min_{t_1, u_1(t), u_C(t)} \int_{t_0}^{t_1} [\frac{\alpha_u}{2} u_1^2(t) + \frac{\alpha_u}{2} u_C^2(t) + \alpha_t] dt + \alpha_v[(v_C(t_1) - v_{d,C})^2 + (v_1(t_1) - v_{d,1})^2] \quad (9a)$$

$$s.t.\ (1),\ (2),\ (7c),\ x_1(t_1) = x_C(t_1) + d_H(v_H(t_1)) \quad (9b)$$

Different from (7a), the cost (9a) minimizes travel time, energy, and speed disruption for *both* CAVs 1 and C. In (7) and (8), the cost incurred by CAV 1 is 0 since it travels with constant speed. (9b) ensures that the rear-end safety constraint (4a) is activated by CAV 1's action. Note that (7b) is used in (9b) to eliminate any dependence on $x_H(t)$ and we set $d_H(v_H(t_1)) = \varphi v_H(t_0) + \delta$. Thus, J_3^I is obtained.

The solution to (7) and (9) can be analytically obtained through Hamiltonian analysis similar to the OCPs formulated and solved in [13]. Thus, we omit the details. In summary, the non-cooperative OCP (7), constant acceleration formulation (8), and cooperative OCP (9) provide three different control policies for CAV C. The optimal policy is given as

$$J^I = \min\{J_1^I, J_2^I, J_3^I\}, \quad (10)$$

Consequently, we can also determine the optimal time t_1^* marking the end of Phase I for CAV C.

B. Optimal Trajectory for CAV C in Phase II

The ideal optimal trajectory for CAV C in Phase II to merge ahead of the HDV is obtained by an OCP we term $\mathbf{OCP}_{[t_1^*, t_f]}$, since it shares the same cost function as $\mathbf{OCP}_{[t_0, t_1)}$ in (7a) except for the new time interval. It also shares the vehicle dynamics (1), speed and control limits (2), and (7c) which becomes $t_1^* \le t_f \le T$. $\mathbf{OCP}_{[t_1^*, t_f]}$ differs only in the terminal state constraint which is now the rear-end safety requirement:

$$x_C(t_f) \ge x_H(t_1^*) + v_H(t_1^*)(t_f - t_1^*) + d_H(v_H(t_1^*)) \quad (11)$$

The solution is "ideal" because it assumes the HDV travels at constant speed in (11), hence ignoring any reaction that the human driver might have when detecting the lane changing action of CAV C. In reality, for C to complete this maneuver safely and optimally, C has to estimate the behavior of H and adjust its own trajectory based on H's response. Similarly, H then needs to adjust its trajectory by reacting to C's response. To model this process, we formulate a bilevel optimization problem for each $i = 1, C, H$ in the following three subsections. We emphasize that this problem is solved by CAV C and we describe its structure in Fig. 3.

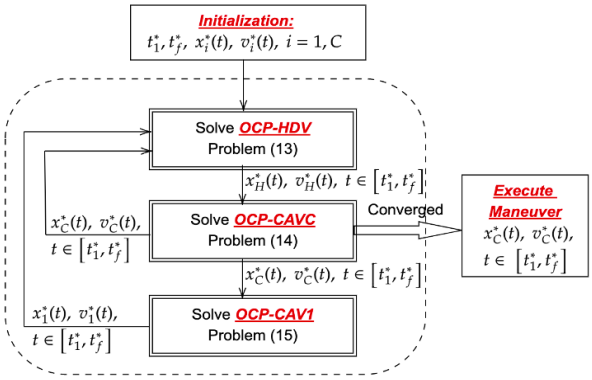

Fig. 3: Bilevel optimization problem solved by CAV C. Initialization consists of solving $\mathbf{OCP}_{[t_0, t_1)}$ to obtain t_1^* and $\mathbf{OCP}_{[t_1^*, t_f]}$ to obtain $t_f^*, x_C^*(t), v_C^*(t)$. In addition, $x_1^*(t) = x_1(t_1^*) + v_1(t_1^*)(t - t_1^*), v_1^*(t) = v_1(t_1^*), t \in [t_1^*, t_f^*]$. Upon convergence, the lane change maneuver is executed with the final $x_C^*(t), v_C^*(t), t \in [t_1^*, t_f^*]$.

*1) Estimate HDV Trajectory (**OCP-HDV**):* We estimate the trajectory of an HDV by assuming that a human driver considers three factors: (i) maintaining a constant speed that minimally deviates from some desired value $v_{d,H}$, (ii) if it needs to change speeds, it does so by minimizing its acceleration/deceleration, which also saves fuel, (iii) guaranteeing its safety (collision avoidance). To model the latter, we define a risk function $s(\cdot)$ as a decreasing function in $x_C(t) - x_H(t)$ since a closer distance between H and C corresponds to a higher collision risk. We adopt a sigmoid function of the form

$$s(x_C(t) - x_H(t)) = 1/(1 + \mu \exp(\mu(x_C(t) - x_H(t) - d))) \quad (12)$$

where μ is adjustable to capture different unsafe regions for different drivers. One can also adjust d to define the size of the unsafe region.

We can now formulate **OCP-HDV** as the problem whose solution is the estimated trajectory that CAV C uses in adjusting its own response by updating $u_C(t)$:

$$\min_{u_H(t)} \int_{t_1^*}^{t_f^*} [\frac{\beta_u}{2} u_H^2(t) + \beta_v (v_H(t) - v_{d,H})^2 + \beta_s s(x_C^*(t) - x_H(t))] dt \quad (13a)$$

$$s.t.\ (1),\ (2),\ x_1^*(t) - x_H(t) \ge d_H(v_H(t)),\ \forall t \in [t_1^*, t_f^*] \quad (13b)$$

where $\beta_{\{u,v,s\}}$ are the non-negative appropriately normalized weights that describe the characteristics of the HDV, i.e., the behavior of the driver. Constraint (13b) denotes the safety constraint between the HDV and its current preceding vehicle CAV 1 for all $t \in [t_1^*, t_f^*]$. We immediately note that $x_C^*(t)$ and $x_1^*(t)$ are unknown to the HDV (except in the first iteration in Fig. 3 where the initial "ideal" trajectories are used). In fact, these are determined by the two lower-level problems (14) and (15) defined next, in response to the HDV's behavior expressed through $x_H^*(t), v_H^*(t),\ t \in [t_1^*, t_f^*]$ from (13).

*2) Update CAV C Trajectory (**OCP-CAVC**):* Similar to **OCP-HDV**, we formulate a bilevel optimization problem

OCP-CAVC for CAV C:

$$\min_{u_C(t)} \int_{t_1^*}^{t_f^*} \frac{\alpha_u}{2} u_C^2 dt + \alpha_v (v_C(t_f^*) - v_{d,C})^2 \tag{14a}$$

$$s.t.\ (1),\ (2), \quad x_C(t_f^*) \geq x_H^*(t_f^*) + d_H(v_H^*(t_f^*)) \tag{14b}$$

The position $x_H^*(t_f^*)$ in the safety constraint (14b) is the optimal terminal position of H given by (13). Problem (14) then provides the best response strategy of CAV C and determines $x_C^*(t), v_C^*(t), u_C^*(t), t \in [t_1^*, t_f^*]$. Note that this information can now be provided to **OCP-HDV** and **OCP-CAV1** as shown in Fig. 3.

*3) Update CAV 1 Trajectory (**OCP-CAV1**):* Since CAV 1 is cooperating with CAV C, CAV 1's strategy is based on the optimal policy of CAV C by applying a similar bilevel optimization problem **OCP-CAV1**:

$$\min_{u_1(t)} \int_{t_1}^{t_f^*} \frac{\alpha_u}{2} u_1^2(t) dt + \alpha_v (v_1(t_f^*) - v_{d,1})^2 \tag{15a}$$

$$s.t.\ (1),\ (2), \quad x_1(t_f^*) - x_C^*(t_f^*) \geq d_C(v_C^*(t_f^*)). \tag{15b}$$

The position $x_C^*(t_f^*)$ in the safety constraint (15b) is the optimal terminal position of C from **OCP-CAVC**. The solution of (15) provides the optimal trajectories $x_1^*(t), v_1^*(t), u_1^*(t), t \in [t_1^*, t_f^*]$ for CAV 1. Note that this information can now be provided to **OCP-HDV** as shown in Fig. 3.

4) Iterated Best Response: The solution to each of the problems (13), (14) and (15) is complicated by the fact that it is coupled to the others through safety constraints or the safety cost. Nonetheless, the problems can be jointly solved through an iterated best response (IBR) process [17] as shown in Fig. 3 to obtain a Nash equilibrium and the corresponding optimal trajectory of vehicle $i = 1, C, H$, $x_i^*(t), v_i^*(t), t \in [t_1^*, t_f^*]$. This, in turn, provides the optimal cost of all three vehicles for Phase II, J^{II}. Combining this with J^I in (10) yields the optimal cost of the CAV C policy "merge ahead of HDV", $J_{C,H} = J^I + J^{II}$.

Note that problems (14) and (15) can be solved analytically through standard Hamiltonian analysis as in [13]. The solution of (13) is complicated by the presence of the nonlinear safety function, but can be numerically solved.

IBR convergence. The convergence of the IBR process in Fig. 3 is generally hard to establish. However, the specific structure of the problems here facilitates such analysis. In particular, convergence depends on the initial states of the vehicles. Since the process starts with (13), observe that its solution depends on $x_1^*(t)$ only through the constraint (13b) and on $x_C^*(t)$ through the risk function $s(x_C(t) - x_H(t))$. Therefore, if the distance between vehicles 1 and H is larger than the minimum safety distance of the HDV, constraint (13b) remains inactive so that the dependence on $x_1^*(t)$ is eliminated. Similarly, if C's speed is greater than H at t_1, their relative distance will increase and the value of $s(x_C(t) - x_H(t))$ becomes zero, leading to the solution of (13) becoming independent of $x_C^*(t)$ as well, hence also leading to the convergence of the iteration process. Conversely, if vehicles 1 and H are close, or the speed of the HDV exceeds that of C, the dependence on $x_1^*(t)$ and $x_c^*(t)$ may not vanish, hence reducing the convergence rate. In this case, however, as we will see next, the optimal action of CAV C becomes that of merging ahead of CAV 1, thus rendering the IBR process irrelevant.

Formal convergence analysis of the IBR process has yet to be carried out. In practice (see Section V), to implement the IBR process, we predetermine a maximum number of iterations N and an error tolerance ε. If convergence within ε has not been attained after N iterations, we relax the terminal time t_f^* and repeat the process. If the terminal time exceeds the upper bound T, we end the process and apply the final $u_C^*(t)$ as the CAV C control.

IV. CAV C MERGES AHEAD OF CAV 1

In this section, we consider the alternative CAV C policy to merge ahead of CAV 1 rather than the HDV. We immediately see that if this policy leads to an optimal cost $J_{C,1}$ such that $J_{C,1} \leq J_{C,H}$, this makes it not only optimal but also independent of the HDV behavior since the HDV's action cannot affect CAV C and the HDV is limited to maintaining a safe distance from CAV 1.

The optimal trajectory, in this case, is obtained jointly with that of the cooperating CAV 1 by solving the problem:

$$\min_{t_f, u_1(t), u_C(t)} \int_{t_0}^{t_f} [\frac{\alpha_u}{2}(u_1^2(t) + u_C^2(t)) + \alpha_t] dt + \frac{\alpha_v}{2}[(v_C(t_f) - v_{d,C})^2 + (v_1(t_f) - v_{d,1})^2] \tag{16a}$$

$$s.t.\ (1),\ (2), \quad x_C(t_f) - x_1(t_f) = d_1(v_1(t_f)). \tag{16b}$$

where $\alpha_{\{t,u,v\}}$ are adjustable properly normalized weights for travel time, energy, and speed deviation, respectively. A solution for t_f^* and $x_i^*(t), v_i^*(t), u_i^*(t), i = 1, C$ for $t \in [t_0, t_f^*]$ can be analytically obtained (omitted here, but shown in the extended version of this paper in [18]). The corresponding cost is denoted by $J_{C,1}$. Clearly, if $J_{C,1} \leq J_{C,H}$ then CAV C selects this policy which depends only on the cooperation between CAVs 1 and C, thus making it *independent of the HDV's behavior*. Lastly, in this case, the HDV trajectory is estimated using (13) with $\beta_s = 0$, since CAV C would not merge ahead of the HDV.

Optimal threshold policy. Observe that $J_{C,H}$ is clearly independent of $x_1(t_1) - x_H(t_1)$, while $J_{C,1}$ is monotonically increasing in $x_1(t_1) - x_H(t_1)$ since CAV C needs to spend more time and energy to merge ahead of CAV 1 as its distance from CAV 1 increases, while CAV 1 may also need to decelerate to decrease C's travel time, which leads to a higher total cost in (15). Therefore, there exists a threshold θ such that if $x_1(t_1) - x_H(t_1) \leq \theta$, CAV C chooses the policy "merge ahead of CAV 1" which is *independent of the HDV's behavior* (see Fig. 4). Conversely, if $x_1(t_1) - x_H(t_1) > \theta$, CAV C chooses "merge ahead of H". In this case, since $x_1(t_1) - x_H(t_1)$ is relatively large, the interaction between H and CAV C is minimal (i.e., the constraint (13b) remains inactive and the value of $s(x_C(t) - x_H(t))$ is near zero so that once again CAV C's optimal trajectory is *robust to the HDV behavior*. An analytical determination of the threshold value is the subject of ongoing work, but it can also be numerically determined as seen in Figs. 4, 5(a).

V. SIMULATION RESULTS

This section provides simulation results illustrating the time and energy-optimal lane-changing trajectories for the CAVs in mixed traffic and demonstrates the threshold-based nature of the optimal policy selection for CAV C. Our simulation setting is that of Fig.1. The allowable speed and acceleration ranges are $v \in [15, 35]m/s$ and $u \in [-7, 3.3]m/s^2$ respectively. The desired speed for the CAVs is set to $30m/s$, while HDV's desired speed is assumed to be the same as its initial speed. To guarantee safety, the inter-vehicle safe distance is given by $\delta = 1.5m$, and the reaction time is $\varphi = 0.6s$. The disruption in (5c) is evaluated with parameters $\gamma_x = 0.2, \gamma_v = 0.8$. When any of the problems (13), (14) and (15) is infeasible or the IBR process has not converged, we relax the terminal time with the relaxation rate $\lambda = 1.8$. The numerical solutions to the optimization problems are obtained using an interior point optimizer (IPOPT) on an Intel(R) Core(TM) i7-8700 3.20GHz.

"Merge ahead of HDV" policy. As discussed in Section III, for C to evaluate the cost of this policy, it breaks down its trajectory into two phases if its initial position is behind H. Thus, in Phase I, we solve problems (7), (9) and (8) to obtain the minimum cost, hence the optimal Phase I trajectory. The weights $\alpha_{\{t,u,v\}}$ in the cost functions are set to 0.55, 0.2, and 0.25, respectively. The maximum maneuver time is set to $T = 15s$. If any of the OCPs is infeasible in this phase, its corresponding cost is set to "Inf". The results are shown in Table. I, where we see that, with these particular parameter settings, it is optimal for C to travel with constant acceleration and $t_1^* = 3.54s$. Proceeding to Phase II, we now solve problems (13), (14) and (15) and carry out the IBR process in Fig. 3. The weights for **OCP-HDV** in (13a) are set to $\beta_u = 0.9, \beta_v = 0.1, \beta_s = 0.1$ and $\mu = 1, d = 0$ in (12) when C is in the unsafe region of H. We set the maximum number of iterations for the IBR process to $N = 5$ and the error tolerance $\varepsilon = 0.01$.

TABLE I: Vehicle C Sample Results in Phase I.

OCPs \ States	$X_C(t_0)$ [m, m/s]	$X_1(t_0)$ [m, m/s]	$X_H(t_0)$ [m, m/s]	cost I	t_1 [s]
(7)	[0,23]	[30,28]	[10,26]	Inf	Inf
(9)	[0,23]	[30,28]	[10,26]	2.99	4.18
(8)	[0,23]	[30,28]	[10,26]	2.73	3.54

"Merge ahead of CAV 1" policy. CAV C evaluates the cost of this policy by solving problem OCP (16).

Computational cost. We considered the "worst case" from a computational cost perspective and solved this problem numerically: our results took an average of 204 ms. We also note that the OCPs (13), (14), (15) each took an average of 50 ms to solve.

TABLE II: Vehicle C sample results for complete maneuvers

Cases \ States	$X_C(t_0)$ [m, m/s]	$X_1(t_0)$ [m, m/s]	$X_H(t_0)$ [m, m/s]	cost	t_f [s]	$d_{H,1}$ [m]
C merges ahead of HDV	[0,23]	[30,28]	[10,26]	4.47	5.74	27.07
C merges ahead of CAV 1	[0,23]	[30,28]	[10,26]	6.84	6.06	27.07
C merges ahead of HDV	[0,24]	[20,28]	[0,24]	4.37	3.41	20
C merges ahead of CAV 1	[0,24]	[20,28]	[0,24]	3.99	5.29	20

The total costs and maneuver time are summarized in Table II. We can see that the optimal policy depends on $d_{H,1} := x_1(t_1) - x_H(t_1)$: as expected when this distance decreases (from 27.07 to 20), it becomes optimal for CAV C to merge ahead of CAV 1; otherwise, it is optimal to merge ahead of H, in which case the gap between CAV 1 and HDV is large enough for C to execute an optimal maneuver.

A. Optimal CAV C policy subject to traffic disruption

In this section, we demonstrate how C can use a simple threshold criterion to determine an optimal policy while also taking into account the traffic disruption metric (5c). We omit Phase I so as to focus on the maneuver phase that includes interactions between the HDV and the two CAVs. The initial states are set as the same with the last two rows in Table. II. The weights are set as $\alpha_u = 0.2$, $\alpha_v = 0.8$,$\beta_u = 0.9, \beta_v = 0.1$. Fixing $\beta_s = 0.1$, $\mu = 1$, the threshold-based optimal policy determination is illustrated in Fig. 4.

Figure 5(a) is similar to Fig. 4 and is intended to explore the effect on the cost $J_{C,H}$ of the parameters $\beta_s, v_{d,H}, \mu$, which characterize the HDV behavior. We see that when β_s increases, the total cost $J_{C,H}$ will also increase because a larger β_s corresponds to a more conservative driver. The parameter μ represents how HDV defines its safe region, which decreases as μ increases. Hence, decreasing μ causes the cost to increase. In Fig. 5(b), we see that "merge ahead of H" (dashed lines) leads to a higher disruption than "merge ahead of CAV 1" (straight line). The reason is that for C to merge ahead of H may require additional deceleration by H. Increasing β_s (the HDV is more conservative) causes H to decelerate and incur a higher disruption. If the HDV aims to reach a higher desired speed $v_{d,H}$, the disruption will obviously also increase according to (5c). Note that "merge ahead of CAV 1" makes HDV's response irrelevant.

B. Comparison with Human-Driven Vehicles

We use the standard car-following models in the SUMO simulator to simulate lane change maneuvers implemented by HDVs (baseline) for a total simulation length of 80 seconds, repeated 9 times. Vehicles 1 and H are defined as C's left leader and follower when C starts to change its lane. The comparison of costs and disruptions is shown in Table III, in which the Baseline results are the average over multiple observed maneuvers. Using the same initial states as Baseline, in this particular case C "merges ahead of H" provides a lower cost and shorter maneuver time than "merge ahead of CAV 1", while causing extremely small disruptions to the HDV (hence also all traffic that follows it). As expected, the "merge ahead of CAV 1" policy causes no disruptions to the HDV. The presence of the two optimally cooperating CAVs can save more than 80% in cost while also causing virtually no disruption to the fast lane traffic.

TABLE III: Cost, Disruption and Maneuver Time Comparison with a Baseline of HDVs only

Scenarios	TotalCost	HDV disruption	Maneuver Time [s]
Baseline	22.37	678.05	7.38
C merges ahead of H	2.85	0.17	2.92
C merges ahead of 1	3.92	0	6.39

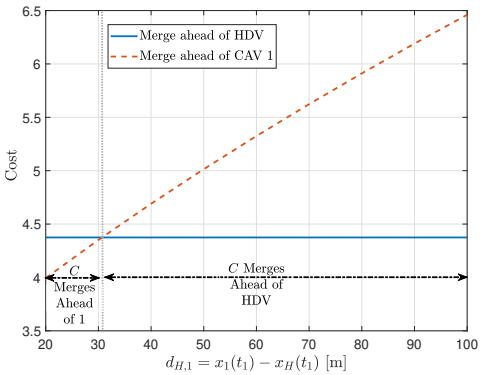

Fig. 4: Optimal policy determination for CAV C. When $d_{H,1}$ increases from $20m$ to $40m$, the optimal policy for CAV C switches from "merge ahead of CAV 1" to "merge ahead of HDV" if C aims to complete a minimal cost maneuver without taking disruption into account.

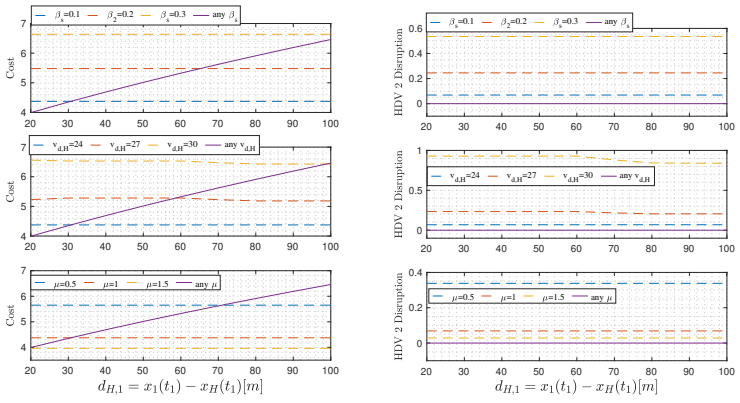

(a) Total cost under different parameters $\beta_s, v_{d,H}, \mu$ (b) Disruption of HDV under different parameters $\beta_s, v_{d,H}, \mu$

Fig. 5: Cost and disruption comparison. Except for the varying parameter in each plot, the other parameters are given by: (i) Two top plots: $v_{d,H} = 24m/s, \mu = 1$, (ii) Two middle plots: $\beta_s = 0.1, \mu = 1$, (iii) Two bottom plots: $\beta_s = 0.1, v_{d,H} = 24m/s$.

VI. CONCLUSIONS AND FUTURE WORK

We have derived optimal control trajectories for a CAV to complete a lane change maneuver in mixed traffic . Vehicle interactions and cooperation have been considered to help optimally perform the maneuver with a simple threshold-based policy. We have shown that CAV cooperation can eliminate or greatly reduce the interaction between CAVs and HDVs. Simulation results show the effectiveness of the proposed controllers and their advantages over a baseline of traffic consisting of HDVs only. Our ongoing work aims at formalizing the threshold-based policy and analytically determining the optimal threshold to use. Moreover, since we are assuming that the objectives and dynamics of HDVs are known to CAVs, future work is directed at improving ways to predict the behavior of human drivers, provide incentives for them to cooperate with CAVs.

REFERENCES

[1] Y. Luo, Y. Xiang, K. Cao, and K. Li, "A dynamic automated lane change maneuver based on vehicle-to-vehicle communication," *Transportation Research Part C: Emerging Technologies*, vol. 62, pp. 87–102, 2016.

[2] D. Zhao, X. Huang, H. Peng, H. Lam, and D. J. LeBlanc, "Accelerated evaluation of automated vehicles in car-following maneuvers," *IEEE Transactions on Intelligent Transportation Systems*, vol. 19, no. 3, pp. 733–744, 2017.

[3] B. Li, Y. Zhang, Y. Feng, Y. Zhang, Y. Ge, and Z. Shao, "Balancing computation speed and quality: A decentralized motion planning method for cooperative lane changes of connected and automated vehicles," *IEEE Transactions on Intelligent Vehicles*, vol. 3, no. 3, pp. 340–350, 2018.

[4] S. He, J. Zeng, B. Zhang, and K. Sreenath, "Rule-based safety-critical control design using control barrier functions with application to autonomous lane change," in *2021 American Control Conference (ACC)*. IEEE, 2021, pp. 178–185.

[5] B. Li, Y. Zhang, Y. Ge, Z. Shao, and P. Li, "Optimal control-based online motion planning for cooperative lane changes of connected and automated vehicles," in *2017 IEEE/RSJ International Conference on Intelligent Robots and Systems (IROS)*. IEEE, 2017, pp. 3689–3694.

[6] Y. Zheng, S. E. Li, K. Li, and W. Ren, "Platooning of connected vehicles with undirected topologies: Robustness analysis and distributed h-infinity controller synthesis," *IEEE Transactions on Intelligent Transportation Systems*, vol. 19, no. 5, pp. 1353–1364, 2017.

[7] L. Zhao, A. Malikopoulos, and J. Rios-Torres, "Optimal control of connected and automated vehicles at roundabouts: An investigation in a mixed-traffic environment," *IFAC-PapersOnLine*, vol. 51, no. 9, pp. 73–78, 2018.

[8] W. Schwarting, A. Pierson, J. Alonso-Mora, S. Karaman, and D. Rus, "Social behavior for autonomous vehicles," *Proceedings of the National Academy of Sciences*, vol. 116, no. 50, pp. 24 972–24 978, 2019.

[9] C. Burger, J. Fischer, F. Bieder, Ö. Ş. Taş, and C. Stiller, "Interaction-aware game-theoretic motion planning for automated vehicles using bi-level optimization," in *2022 IEEE 25th International Conference on Intelligent Transportation Systems*. IEEE, 2022, pp. 3978–3985.

[10] M. Wang, Z. Wang, J. Talbot, J. C. Gerdes, and M. Schwager, "Game theoretic planning for self-driving cars in competitive scenarios." in *Robotics: Science and Systems*, 2019.

[11] L. Guo and Y. Jia, "Inverse model predictive control (impc) based modeling and prediction of human-driven vehicles in mixed traffic," *IEEE Trans. on Intelligent Vehicles*, vol. 6, no. 3, pp. 501–512, 2020.

[12] V.-A. Le and A. A. Malikopoulos, "A cooperative optimal control framework for connected and automated vehicles in mixed traffic using social value orientation," in *2022 IEEE 61st Conference on Decision and Control (CDC)*. IEEE, 2022, pp. 6272–6277.

[13] R. Chen, C. G. Cassandras, A. Tahmasbi-Sarvestani, S. Saigusa, H. N. Mahjoub, and Y. K. Al-Nadawi, "Cooperative time and energy-optimal lane change maneuvers for connected automated vehicles," *IEEE Transactions on Intelligent Transportation Systems*, vol. 23, no. 4, pp. 3445–3460, 2020.

[14] K. Xu, C. G. Cassandras, and W. Xiao, "Decentralized time and energy-optimal control of connected and automated vehicles in a roundabout," in *2021 IEEE International Intelligent Transportation Systems Conference*. IEEE, 2021, pp. 681–686.

[15] K. Vogel, "A comparison of headway and time to collision as safety indicators," *Accident Analysis & Prevention*, vol. 35, no. 3, pp. 427–433, 2003.

[16] A. S. C. Armijos, A. Li, C. G. Cassandras, Y. K. Al-Nadawi, H. Araki, B. Chalaki, E. Moradi-Pari, H. N. Mahjoub, and V. Tadiparthi, "Cooperative energy and time-optimal lane change maneuvers with minimal highway traffic disruption," *arXiv:2211.08636*, 2022.

[17] Z. Wang, T. Taubner, and M. Schwager, "Multi-agent sensitivity enhanced iterative best response: A real-time game theoretic planner for drone racing in 3d environments," *Robotics and Autonomous Systems*, vol. 125, p. 103410, 2020.

[18] A. Li, A. S. C. Armijos, and C. G. Cassandras, "Cooperative lane changing in mixed traffic can be robust to human driver behavior," *arXiv:2303.16948*, 2023.